

Review

# Recent Developments in Modulation Spectroscopy for Methane Detection Based on Tunable Diode Laser

Fei Wang , Shuhai Jia <sup>\*</sup>, Yonglin Wang and Zhenhua Tang 

Department of Mechanical Engineering, Xi'an Jiaotong University, Xi'an 710049, China

<sup>\*</sup> Correspondence: shjia@mail.xjtu.edu.cn; Tel.: +86-131-5206-8353

Received: 30 April 2019; Accepted: 11 July 2019; Published: 15 July 2019



**Abstract:** In this review, methane absorption characteristics mainly in the near-infrared region and typical types of currently available semiconductor lasers are described. Wavelength modulation spectroscopy (WMS), frequency modulation spectroscopy (FMS), and two-tone frequency modulation spectroscopy (TTFMS), as major techniques in modulation spectroscopy, are presented in combination with the application of methane detection.

**Keywords:** methane; tunable diode laser; wavelength modulation spectroscopy; frequency modulation spectroscopy; two-tone frequency modulation spectroscopy

## 1. Introduction

Due to global warming and climate change, the monitoring and detection of atmospheric gas concentration has come to be of great value. Although the average background level of methane (CH<sub>4</sub>) (~1.89 ppm) in the earth's atmosphere is roughly 200 times lower than that of CO<sub>2</sub> (~400 ppm), the contribution of CH<sub>4</sub> to the greenhouse effect per mole is 25 times larger than CO<sub>2</sub> [1,2]. Therefore, a fast, accurate, and precise monitoring of trace greenhouse gas of CH<sub>4</sub> is essential. There are some methods for detecting methane, including chemical processes [3–6] and optical spectroscopy [7–9]. Optical spectroscopy for detecting gases is based on the Beer-Lambert law [10–12], in which the light attenuation is related to the effective length of the sample in an absorbing medium, and to the concentration of absorbing species, respectively. By this theory, the emission wavelength of the narrow-linewidth diode laser is scanned over the target gas absorption line, and tunable diode laser absorption spectroscopy (TDLAS) has become an effective technique for the rapid and online analysis of gas component concentration, due to the advantage of high spectrum resolution [13–22]. Direct detection and wavelength modulation spectroscopy are the most common sensing methods of TDLAS [23,24]. Comparatively speaking, wavelength/frequency modulation spectroscopy is less vulnerable to the effects of background noise and more suitable for detecting trace gases. Moreover, modulation spectroscopy is widely used for the detection of various gases with the advantage of high signal-to-noise ratio (SNR) [25,26]. Wavelength modulation spectroscopy (WMS), frequency modulation spectroscopy (FMS), and two-tone frequency modulation spectroscopy (TTFMS) are the main techniques in modulation absorption spectroscopy. Since each technique has its strengths and weaknesses, they have also been applied for detecting methane depending on the situation.

In this review, after introducing methane absorption characteristics and recent progress of tunable diode lasers (TDLs), recent advances in methane detection using modulation spectroscopy are presented.

## 2. Methane Absorption Lines

The CH<sub>4</sub> molecule has a spherical top, and belongs to the tetrahedral point family. It exhibits four fundamental vibration modes:  $\nu_1 = 2913 \text{ cm}^{-1}$ ,  $\nu_2 = 1533.3 \text{ cm}^{-1}$ ,  $\nu_3 = 3018.9 \text{ cm}^{-1}$  and

$\nu_4 = 1305.9 \text{ cm}^{-1}$  [27]. Of these, the two bending vibrations are  $\nu_2$  (asymmetric) and  $\nu_4$  (symmetric), while  $\nu_1$  (symmetric) and  $\nu_3$  (asymmetric) are the two stretching vibrations [28]. The successive resonance spacing is about  $1500 \text{ cm}^{-1}$  [29]. In the near-infrared region (1100–1800 nm), the  $2\nu_3$  band near 1670 nm and the  $\nu_2 + 2\nu_3$  band near 1300 nm are primary overtone rotational-vibrational combination bands.

Based on the Beer-Lambert law (Equation (1)) [10,11], many laser absorption spectroscopy techniques are applied to measure gas concentration, including WMS, FMS, and TTFMS.

$$\tau(\nu) = \frac{I_t(\nu)}{I_o(\nu)} = e^{-\sigma(\nu)xL} = e^{-\alpha(\nu)} \quad (1)$$

where,  $\tau(\nu)$  represents the transmittance of light,  $I_o(\nu)$  and  $I_t(\nu)$  represent the incident and transmitted intensities of a certain wavelength, respectively,  $\sigma(\nu)$  represents the cross-section of gas absorption at a certain wavelength,  $x$  represents the gas concentration, and  $L$  represents the length of the path that the light travels through absorbing media,  $\alpha(\nu)$  represents the transmission coefficient. In absorption spectroscopy, the detection sensitivity is related to the length of the absorption path and the absorption line intensity of molecule, respectively [2].

According to differences in measurement area and monitoring technique, different frequency bands involving methane transitions from near infrared to mid infrared have been applied [30]. With the development of near-infrared light sources and fiber technology, the corresponding test system in the near infrared region is more mature [31–33]. Washenfelder et al. [34] investigated that the absorption strengths of the  $2\nu_3$  band were suitable for providing high sensitivity for ground-based high-resolution spectrometry in the near-infrared spectrum. The absorption intensity of  $\text{CH}_4$  in the  $2\nu_3$  band is more than four orders of magnitude stronger than that of  $\text{H}_2\text{O}$  and  $\text{CO}_2$ , which can be safely neglected [35]. The related spectroscopic parameters of  $2\nu_3$  band, including line positions, line intensities, line widths, line shifts, and line couplings are certain, as described in reference [36–41].

### 3. Tunable Diode Laser

Semiconductor diode lasers are mainly made of gallium arsenic (GaAs), aluminum (GaAlAs), indium phosphite (InGaAlP, InGaAs or InGaP) and lead salt [42,43]. Moreover, diode lasers are frequently used for modulation spectroscopy because of fast tunability of laser wavelength and fast response times [44,45]. Compared with the spatial characteristics, the spectral characteristics of lasers, such as linewidth and tunability, are more valuable in modulation spectroscopy. To ensure high-quality measurement, narrow line widths, single frequency emission and the inherent stability of the laser are of importance.

The longitudinal mode spacing is relatively narrow, and the oscillation bands of the laser exist in many longitudinal modes. Therefore, the distributed Bragg reflection (DBR) and distributed feedback (DFB) lasers are common diode lasers in the near-infrared spectral region, in which the feedback necessary for the lasing action is distributed throughout the cavity length, and the longitudinal mode selection is improved [46–48]. Such lasers covering the absorption bands of  $\text{CH}_4$  at 1650 nm have been applied for detecting methane gas [49]. Recently, quantum well (QW) DFB lasers have generated the emission wavelengths of  $2.6 \mu\text{m}$  [50] and  $3.4 \mu\text{m}$  [51,52]. Nevertheless, the overtone and combination bands of many target molecules are in the near infrared region, which is strong enough to get ppm, even ppb detection levels [13].

Depending on the laser materials, commercial diode lasers can be classified into two generic groups: gallium arsenide-based lasers with wavelengths below  $3 \mu\text{m}$ , and lead salt-based lasers with wavelengths above  $3 \mu\text{m}$ , which are usually fabricated from semiconductor materials in groups of III-V and IV-VI, respectively [53]. Among them, the laser beams of lead-salt diode lasers can range from 3 to  $30 \mu\text{m}$ , covering the fundamental transitions of most atmospheric trace gases, which is in the mid-infrared region. Therefore, lead-salt diode lasers are appropriate for spectroscopic gas detection in

theory. However, some drawbacks, such as instability in single mode operation, low output power, and high costs, result in their limited practical application in comparison to GaAs lasers [54,55].

Mid-infrared wavelength band covers the fundamental bands of most gas molecules. Therefore, many researchers are carrying out studies with the aim of improving the performance of mid-infrared lasers or develop new type lasers for higher sensitivity. For example, a diode laser with the external cavity (EC) (e.g., Littrow or Littman-Metcalf configuration) has been proposed to be tuned over a broad spectral range, which is called an external cavity diode laser (ECDL) [56]. However, mode hops limit more improvements of spectral range in a single scan [57]. By contrast, Interband cascade lasers (ICLs) [58] in the 2.5–4  $\mu\text{m}$  wavelength range and quantum cascade lasers (QCLs) [59] in the 4–12  $\mu\text{m}$  wavelength range can provide continuous-wave (CW) output power levels with low input powers. Due to the use of interband transitions, the laser action of ICLs can be obtained at lower electrical input powers than QCLs. However, the phonon interactions in ICLs typically occur on a much slow time scale, which is slower than the longitudinal optical phonon interactions in QCLs. QCLs are widely used as the convenient spectroscopic source to trace gas analysis. In addition, a significant advance in mid-infrared spectroscopic detection has been made, due to their room temperature operation, inherently narrow linewidth and high output power [60–63]. It is worth pointing out that the linewidth reduction of QCLs is achieved by frequency locking to resonant cavities [64]. Recently, an EC configuration is adopted to further improve the performance of QCLs [65,66], and rapid wavelength modulation can be achieved by directly modulating the injection current of QCL chip. A wide tuning range between 7960 and 8840 nm can be performed by continuous-wave operation of EC QCL [67].

#### 4. Application of Modulation Spectroscopy for Methane Detection

Due to the advantage of high spectral resolution, TDLAS has been widely used to measure methane absorptions and concentrations in the applications of molecular spectroscopy [68], natural gas leak detection [69], and trace greenhouse gas monitoring [70] and so on. With TDLAS, the laser frequency is scanned across the absorption line of methane gas, by tuning the output wavelength of the diode laser. Many methane sensor systems are developed utilizing modulation spectroscopy [71,72] to improve the limits of methane detection. The modulation spectroscopy technique used for TDLAS has been reviewed in detail elsewhere [29,44,73,74], and this section aims to bring relevant methane detection based on modulation spectroscopy up to date with recent developments.

##### 4.1. Wavelength Modulation Spectroscopy Applied for Methane Detection

###### 4.1.1. Principle of Wavelength Modulation Spectroscopy

In a typical TDLAS with WMS, the laser frequency is modulated by applying a low-frequency ramp and a high-frequency sine wave [23,70]. After interacting with the absorption line of the target gas, the modulated light generates the signals at different harmonics of modulation frequency [75]. At a fixed harmonic, the amount of signal attenuation is proportional to the gas absorption, and the modulated wavelength is demodulated by a phase-sensitive detector [76]. The demodulated wavelength at a particular harmonic  $nf$  ( $n = 2, 3, 4$ , etc.) is usually directed for the detection, and the detection bandwidth is shifted to higher frequencies, where  $1/f$  noise is smaller. The output spectrum of the laser modulated by a radio frequency is shown in Figure 1 [77].

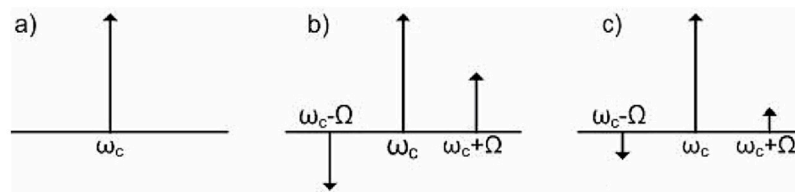


**Figure 1.** The spectral output of the laser at a radio frequency: (a) unmodulated; (b) modulated with no absorption; (c) modulated with absorption.  $\omega_c$  and  $\omega_c \pm \Omega$  represent the carrier frequency and the side band frequencies, respectively;  $\Omega$  represents the frequency of the laser. Reproduced with permission from [77], the Institute of Electrical and Electronics Engineers, 2008.

#### 4.1.2. Near Infrared Methane Detection Systems Based on WMS

Based on TDLs with WMS, researchers have successfully studied many high-performance methane detection systems in the near infrared region [71,72,78,79]. Typically, a DFB laser is often used as a light source. A portable methane detection device was developed by using a DFB diode laser centered at 1.654  $\mu\text{m}$  [71]. The second harmonic wavelength modulation spectroscopy (2f-WMS) was adopted. Within the detection range of 0–10<sup>6</sup> ppm, the relative detection error was less than 7%. Liu et al. [72] also designed a trace methane gas sensor. The frequency modulation technology was applied in WMS to move the bandwidth of detection from low frequency to high frequency, to reduce 1/f noise. Zheng et al. [78] described a portable CH<sub>4</sub> detection sensor. The temperature of the DFB laser was controlled by a software-based proportion-integration-differentiation (PID) algorithm. In addition, the measurement range was from 0 to 100%. Then, the absorption length was added from 0.2 m to 0.4 m, and an open gas sensing probe was set in an improved system [79]. In the lab group's previous reports, the two mid-infrared detection sensors had been developed [80,81]. Though the near-infrared sensor has a longer effective path length of the gas cell, the mid-infrared sensor has a higher MDL of 5 ppm. This is due to the fact that the absorption line intensity at 3.31  $\mu\text{m}$  is stronger over two orders than that at 1.65  $\mu\text{m}$ . The wavelet-denoising (WD)-assisted wavelength modulation technique is successfully suppressing the noise in mid-infrared detection sensors. A sequential multipoint sensor applying 2f-WMS technique was firstly developed by Shemshad [82]. The sensor did not use any multiplexing techniques to distribute the laser intensity among a multitude of gas cells.

In some systems, the DFB laser is replaced with a vertical cavity laser (VCL) as a light source [83]. Paige et al. [69] developed a portable natural gas leak detector based on a VCL. The detector could measure methane concentrations from ambient methane levels (1.8 ppm) to pure gas. In the detection process, the response time of the detector was 1–2 s, and the detection precision was below 1%.

Due to the low cost of near-infrared laser and the development of optical communications networks, some instruments in near infrared have been expanded into the commercialized application. The LI-7700 Methane Analyzer (LI-COR Biosciences Lincoln, NE, USA) was developed for detecting methane by eddy covariance method, which had the advantages of light weight, open path, and low power requirement [84]. A tunable diode laser centered at 1.65  $\mu\text{m}$  and a Herriott cell with a 30 m effective path length were employed. The wavelength was modulated across the absorption band at the sub-MHz frequency. Pressure- and temperature-induced changes in line shape and population distribution, changing in laser power and mirror reflectivity as well, were compensated by using computational fitting algorithms. This ensured that measurements remained accurate over a wide range of pressure and temperature conditions. The Laser Gas™ iQ2 analyzer (NEO, AS) was the first all-in-one TDLAS analyzer to measure up to four gases (O<sub>2</sub>, CO, CH<sub>4</sub>, H<sub>2</sub>O) and temperature depending on configuration, which eliminated the need for multiple units for combustion analysis. Then the Laser Gas™ II Open Path (OP) Monitor (NEO, AS), a compact and high-performance gas analyzer, was created for long-distance monitoring in ambient air.

#### 4.1.3. Mid Infrared Methane Detection Systems Based on WMS

Methane detection systems based on the mid-infrared laser have been researched for quite some time. However, traditional mid-infrared sensors have some drawbacks, such as the low power of the laser and the instability of a laser in single mode operation. QCL, as a convenient mid-infrared laser source, is widely employed for methane monitoring at room temperature. A small in situ sensor system was developed to monitor the concentration of CH<sub>4</sub> and N<sub>2</sub>O in real time [85]. The light source was a QCL operating at 7.83 μm. The wavelength was scanned over the absorption lines of CH<sub>4</sub> and N<sub>2</sub>O at different operating temperatures, achieving simultaneous dual-species detection. The sampling volume of the multipass cell was only 225 mL, resulting in the compact size of the system. Moreover, an external cavity quantum cascade laser (EC-QCL), covering the absorption lines of four atmospheric greenhouse gases, was applied in a sensor system [86]. Additionally, gallium antimonite (GaSb)-based ICLs have been used for mid-infrared sensing [87,88]. In addition, the commercial availability of ICLs was achieved in 2009. Ye et al. [87] demonstrated a mid-infrared dual-gas detection system (CH<sub>4</sub> and C<sub>2</sub>H<sub>6</sub>) based on a single ICL [87]. However, the power consumption of ~250 W was relatively high. The weight of the oil-free vacuum pump and pressure controller and readout in the system was heavy. To address the limitations, new portable sensor systems were developed [88,89], in which competitive performances were revealed compared with other reported portable or handheld sensor devices. Mid-infrared sources based on DFG effects are also employed for methane detection. Commercial and off-the-shelf near-infrared lasers are purchased to act as the mixing sources. Armstrong et al. [90] described a mid-infrared methane detection system using the difference frequency generation (DFG) process in a periodically poled lithium niobate (PPLN) crystal. The DFG system was used to implement TDLAS with WMS. The pump wavelength and the signal wavelength were provided by a fiber Bragg grating diode laser and a DFB diode laser, respectively. The fundamental absorption line of methane located around 3.4 μm was addressed. Since then, several researchers have reported more absorption detection applications using DFG processes. A system utilizing a dual-wavelength amplifier for DFG process was firstly presented [91]. As shown in Figure 2, the dual-wavelength amplifier is used to amplify both of pump wavelength and signal wavelength, and simple 2f methane detection is carried out. However, the detectable concentration of methane at the same absorption line is less than achieved by Armstrong I. et al. [90]. The minimum detectable methane concentration was at the level of 26 ppbv for an open-path interaction length of 8 m [92]. Zhao et al. [93] described a single-frequency CW difference-DFG source, which was tunable from 3.1 to 3.6 μm. The output power of the source can reach tens of milliwatts. Therefore, the wideband-tunable mid-infrared source has the potential in the application of trace gas detection.

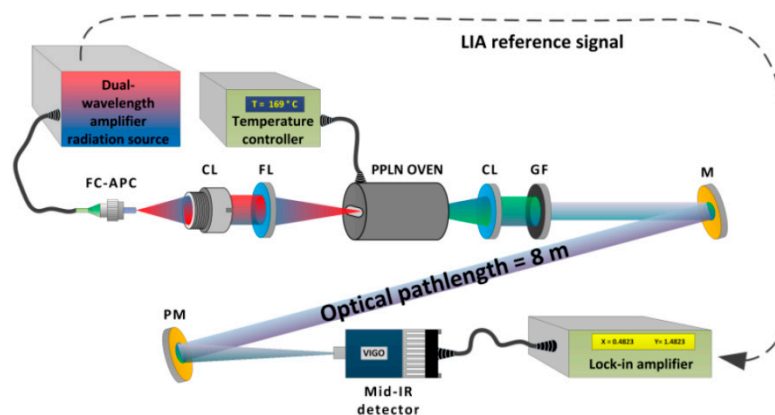


**Figure 2.** The methane detection system based on a dual-wavelength amplifier. Reproduced with permission from [91], Optical Society of America, 2013.

#### 4.1.4. Multi-Mode Diode Laser Applied for Methane Detection Based on WMS

In the above research, almost every light source falls into a single-mode diode laser. The multi-mode diode laser is also used as a light source in some systems. A tunable multi-mode diode laser with a central wavelength of 1318 nm was applied for remote detection of methane by Gao et al. [94]. In the experiment, the multi-mode laser modes merely depended on the input current and temperature, and the tuning range was continual. The reliability of the data analysis process was certificated. Later, Cai et al. [95] reported what was probably the first application of measuring CH<sub>4</sub> and CO by using a multi-mode ECDL emitting around 2.33 μm, as shown in Figure 3. Correlation spectroscopy was used for signals identification and quantitative analysis. Although it is easier to obtain the signal within the tuning range with a multi-mode diode laser than with a single-mode diode laser due to its larger covering area, the mode-jump and mode competition, an intrinsic property of the multi-mode laser, becomes an obstacle to further applications in trace gas detection.

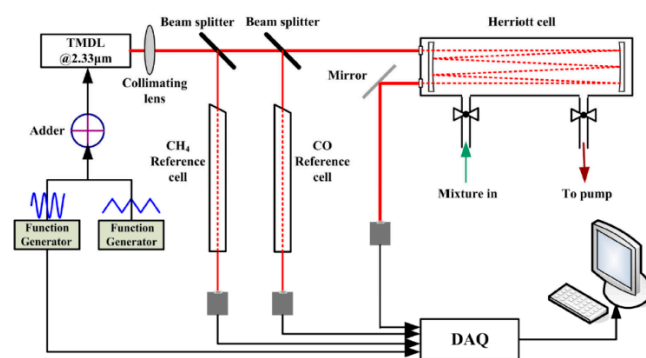


**Figure 3.** The experimental setup used for the simultaneous measurement of CH<sub>4</sub> and CO. Reproduced with permission from [95], Optical Society of America, 2016.

#### 4.1.5. Optimization of Methane Detection Based on WMS

Apart from high detection sensitivity, the capacity of suppressing  $1/f$  noise makes WMS a widely used technique [89,96]. However, optical interference fringe, the primary cause of background fluctuation, has not been effectively suppressed in WMS. Many methods, including the adoption of post-detection filtering and the improvement of the detection system, have been attempted to optimize the optical interference fringe in methane sensors [97]. For example, recently, a method of combining dual tone modulation (DTM) with vibration reflector (VR) was introduced, which decreased the standard deviation (STD) value of the background signal to 0.0924 ppm [98].

Other than the optical interference fringe, some kinds of MPCs, as well as the modulation spectroscopy technique, have also been under study to improve the detection sensitivity, by increasing the effective optical path while at the same time keeping the small size of methane sensor. White cells [99], Herriott cells [100] and Chernin [101] are the three most common MPCs applied for detecting gas, and variations on these have been developed. Liu et al. [2] studied a novel compact dense-pattern multipass cell (DP-MPC). The cell was used to detect atmospheric methane in TDLAS with WMS. Then, a confocal MPC was developed to build a compact and portable methane sensor [102]. The MPC was mainly comprised of confocal mirrors, of which the radii of curvature were 500 mm. Compared to the reported sensors, the sensitivity of ambient methane was improved. Additionally, many other MPCs are also used for the detection of atmospheric trace species, such as a multiple-reflection optical cell with three mirrors [103], the multipass cell formed by two twisted cylindrical mirrors [104] and circular multireflection cell [105]. Some parameters of novel MPCs are listed in Table 1.

**Table 1.** Some parameters of novel multipass cells.

Title of Multipass Cells	Components	Path Length	Detection Limit	Taken from Refs.
Dense-pattern multipass cell	Two silver-coated concave spherical mirrors	26.4 m	<79 ppb	[2]
Confocal multipass cell	A confocal configuration of six mirrors	290 m	1.2 ppb	[102]
Multiple-reflection optical cell	Three mirrors	140.3 m	128 ppb	[103]
Multiple-pass optical cell	Two twisted cylindrical high-reflectivity mirrors	29.5 m	-	[104]
Circular multireflection cell	A polished spherical reflecting surface	105 cm	300 ppm	[105]

## 4.2. Frequency Modulation Spectroscopy Applied for Methane Detection

### 4.2.1. Principle of Frequency Modulation Spectroscopy

FMS is an offshoot of WMS, and the difference between WMS and FMS lies in the magnitude of the modulation frequency. When modulation frequency is larger than the width of the absorption line of interest, the technique is named by frequency modulation (FM). Compared with that of WMS in the  $1/f$  noise dominated region (10 kHz), the modulation frequency of FMS is the 100 kHz range, which is in a shot noise limited domain [29]. When detector quantum noise becomes the limiting factor for the sensitivity of the detection system, the detection limit can be described by Equation (2).

$$SNR = \frac{P_{signal}}{(P_{1/f}^2 + P_{sn}^2 + P_{tn}^2)^{1/2}} \quad (2)$$

wherein,  $P_{1/f}$  represents the detector excess noise,  $P_{sn}$  represents the shot noise of the detector,  $P_{tn}$  represents the detector thermal noise, and  $P_{signal}$  represents the signal proportional to the incident laser power on the detector.

### 4.2.2. Methane Detection Systems Based on FMS

Generally, FMS can be applied for the situation where WMS is applied in reference [106]. Compared with that of WMS, processing electronics or detector of FMS should have a broader bandwidth in order to generate higher frequencies [107]. This is a crucial limitation of FMS. Werle et al. [108] determined that the absorbance of detection using one-tone FMS in a 1-Hz bandwidth could be  $10^{-8}$  when the laser-induced shot noise of detector exceeded thermal noise. However, the power of many lead-salt diode lasers is not sufficient to produce shot-noise-limited spectroscopy. Frequency modulation of GaAlAs lasers was first demonstrated by Rickett et al. [109] in 1980. The method of FM-TDLAS was used by Gulluk et al. [110] to measure  $\text{CO}_2$ ,  $\text{CH}_4$ ,  $\text{N}_2\text{O}$ , and  $\text{CO}$  in air samples of a few  $\text{cm}^3$ . The lead-salt diode laser was tuned at a typical frequency of 1 kHz, and the rf signal of 100–195 MHz was superimposed on the laser current. Then, Pavone et al. [24] used a GaAlAs diode laser (DL) at 886 nm to obtain the sensitivities of three detection techniques in methane sensor in order to more clearly compare WMS and FMS with TTFMS. The laser was tuned on a third overtone methane transition for measuring the minimum detectable absorption. The modulation frequency was 1 kHz, 100 MHz, and  $390 \pm 5$  MHz for WMS, FMS and TTFMS, and the minimum detectable absorptions were  $4.5 \times 10^{-7}$ ,  $9.7 \times 10^{-8}$  and  $6.4 \times 10^{-8}$ , respectively.

Based on FMS, TDLs offer remote detection of methane gas the opportunity to operate over distances of 10 m or more in high sensitivity [111]. In these systems, the laser beam aimed through the probed region is collected after one-way transmission or further reflection from a topographic target [112,113]. The ambient methane detection using the FM technique at a frequency of 5.35 MHz was reported by Uehara et al. [112]. Then, Iseki et al. [113] described a portable methane detection sensor with a 1.65- $\mu\text{m}$  InGaAsP DFB laser. The tuning range of wavelength was  $14\text{ cm}^{-1}$ .

In addition to conventional lasers, new types of lasers such as QCL are also used for FMS in methane detection. Gagliardi et al. [114] developed a novel laser spectrometer, which relied on a QCL for detecting methane and nitrous oxide. Moreover, the research group firstly and thoroughly applied single-tone FM technique to QCL, detecting the same components under low pressure, as shown in Figure 4 [65]. Two QCLs of 8.06  $\mu\text{m}$  and 7.3  $\mu\text{m}$  are applied for FMS on  $\text{N}_2\text{O}$  and TTFMS on  $\text{CH}_4$ , respectively. For methane gas, the minimum detectable concentration can reach up to 400 ppt  $\text{Hz}^{-1/2}$ . Due to the tunability and sensitivity characteristics of the system, a mixture of gases can be monitored. As they summarized, QCL is an appropriate choice for frequency modulation spectroscopy in the mid-infrared region.

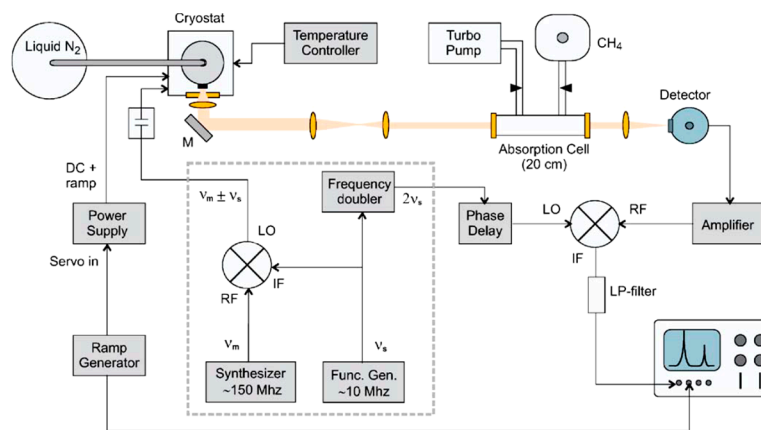


**Figure 4.** Schematic of the experimental set-up based on the FM technique. Reproduced with permission from [65], Springer, 2006.

#### 4.2.3. Optimization of Methane Detection Based on FMS

Some researchers [115–117] have tried to improve the performance of methane sensors based on QCLs in several ways. For example, a fast optical modulation was achieved by introducing an fs NIR pulse train in a typical QCL, which was different from the traditional modulation method by temperature tuning or current injection [115]. The FM was obtained at frequencies up to 1.67 GHz, which was a benefit to get higher sensitivity of detection. Eichholz et al. [116] found out that the FM technique with QCLs at terahertz (THz) frequencies was suitable for high-resolution molecular spectroscopy. Then DFB QCLs, as the radiation source, were used to set up THz spectrometers [116,117]. The investigated molecular parameters such as transition frequency and pressure broadening of  $\text{CH}_3\text{OH}$  were presented.

### 4.3. Two-Tone Frequency Modulation Spectroscopy Applied for Methane Detection

#### 4.3.1. Principle of Two-Tone Frequency Modulation Spectroscopy

The frequency modulation spectroscopy is called single-tone FMS (i.e., Standard FM) or two-tone FMS, depending on the number of modulation tones [107]. The modulation of lasers in TTFMS is completed by a pair of closely spaced frequencies simultaneously, which are  $\omega_1 = \omega_c + \Omega/2$  and  $\omega_2 = \omega_c - \Omega/2$ , respectively. Wherein  $\omega_c$  is the center frequency and  $\Omega$  is the difference frequency. TTFMS has higher modulation frequencies in comparison with FMS. In the TTFM technique, the

advantages of standard FM are used in conjunction with the benefits of a considerable reduction in detection bandwidth, with additional improvement in SNR [107].

#### 4.3.2. Methane Detection Systems Based on TTFMS

In 1982, the TTFM technique was first proposed by Janik et al. [118]. Then modulation frequencies increased from the kHz range to the tens of GHz range due to using a CW dye laser source and an electro-optic modulator [119]. In the same year, the frequency of hundreds of MHz was obtained by using a lead-salt diode laser [120]. Modugno et al. [121] employed a DFB diode laser to develop a TTFMS spectrometer for monitoring methane. A balanced homodyne detection technique was adopted so that the spectrometer had high sensitivity. The modulation frequency and the rf frequency were 2 GHz and 5 MHz, respectively. The sensitivity of the spectrometer was up to  $7(2) \times 10^{-8}$  at a 1-Hz bandwidth. Recently, the TTFMS technique has been used in conjunction with a DFG radiation source. Maddaloni et al. [122] developed a portable DFG spectrometer, as shown in Figure 5. Compared with direct absorption, SNR has been enhanced by a factor of 100 by using TTFMS. Gagliardi et al. [65] described another portable spectrometer based on QCLs and TTFMS for monitoring CH<sub>4</sub>. The wavelength tunability vs. temperature was 2 GHz/K for QCL emitting at 7.3 μm. The output SNR was enhanced about six times than that of direct absorption.

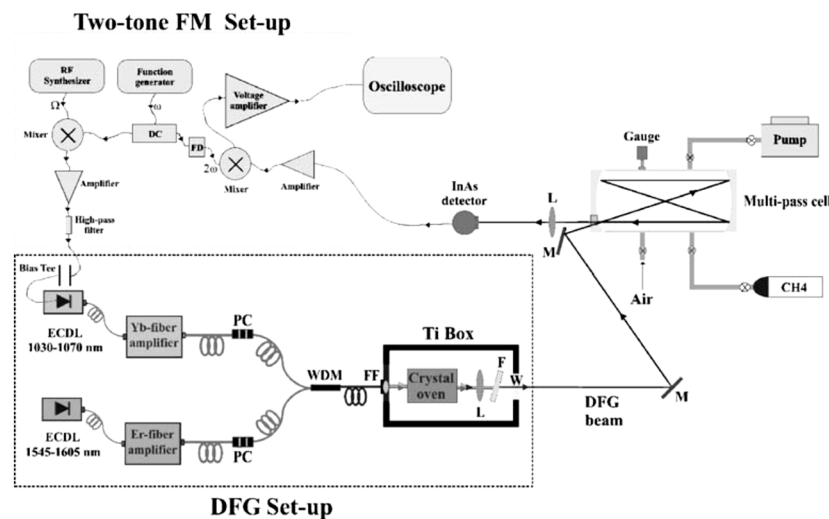


**Figure 5.** Schematic drawing of the experimental set-up of a portable spectrometer. Reproduced with permission from [122], Springer, 2006.

#### 4.3.3. Optimization of Methane Detection Based on TTFMS

In absorption systems based on TTFM technique, optical interference fringe is also a limiting factor for detection sensitivity. A convenient fringe suppression method was employed to improve the sensitivity in a CH<sub>4</sub> detection system, as shown in Figure 6 [70]. Modulation depth optimization and TTFM technology is applied in this system. In addition, the MDL at 1.654 μm is enhanced to 130 ppb.m for a 50-min period. Observed detection sensitivity is given in the conclusion in Table 2.

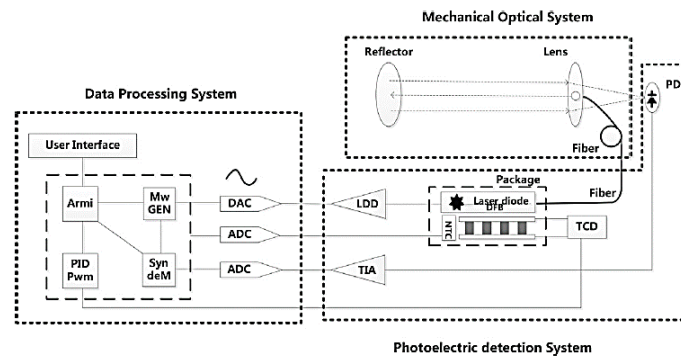


**Figure 6.** Frame diagram of the CH<sub>4</sub> detection system. Reproduced with permission from [70], Elsevier Science, 2017.

**Table 2.** Methane measurement characteristics for modulation spectroscopy techniques.

Spectroscopic Technique	Spectral Wavelength (nm)	Detection Limit/Measured Concentration	Source Type	Sample/Path Length	References
Wavelength Modulation	1318	25 ppm.m	DL	80 cm gas cell	[94]
	1650	1 ppm	VCL	107 cm gas cell	[69]
	1651	1.2 ppb	DFB	290 m gas cell	[102]
	1653	79 ppb	DFB	26.4 m gas cell	[2]
	1654	130 ppb.m <sup>a</sup>	DFB	Open path	[70]
	1654	11 ppm	DFB	0.2 m gas cell	[71]
	1654	1.4 ppm	DFB	76 m gas cell	[72]
	1654	11 ppm	DFB	0.2 m gas cell	[78]
	1654	12 ppm.m <sup>b</sup>	DFB	40 cm gas cell	[79]
	1654	5 ppb	DL	30 m open cell	[84]
	2330	81 ppb	ECDL	100 m gas cell	[95]
	3100	5 ppm	DFB	7.5 cm gas cell	[81]
	3291	2.1 ppmv <sup>c</sup>	ICL	54.6 m gas cell	[88]
	3291	5 ppbv	ICL	54.6 m gas cell	[89]
	3334	17.4 ppbv	ICL	54.6 m gas cell	[87]
3403	1.31 ppm.m	DFB	30 mm gas cell	[90]	
3403	26 ppbv	DFB	Open path	[91]	
7800	2.2 ppbv <sup>d</sup>	QCL	57.6 m gas cell	[86]	
Frequency Modulation	1654	450 ppb.m	DFB	0.2 m gas cell	[113]
	3357	20.3 ppbv	DL	25 cm gas cell	[110]
	7658	20 ppm	QCL	20 cm gas cell	[114]
Two-Tone Frequency Modulation	886	-	DL	1.5 m gas cell	[24]
	3314	3 ppb Hz <sup>-1/2</sup> <sup>e</sup>	ECDL	13 m gas cell	[122]
	3428	30 ppt Hz <sup>-1/2</sup>	ECDL	13 m gas cell	[122]
	7300	-	QCL	20 cm gas cell	[65]

<sup>a</sup> Parts per billion meters (length normalized concentration unit); <sup>b</sup> Parts per million meters; <sup>c</sup> Parts per million by volume; <sup>d</sup> Parts per billion by volume; <sup>e</sup> Parts per billion by the negative square root of Hertz.

### 5. Conclusions

The characteristics of modulation spectroscopy techniques, based on TDLs for detecting methane in the last decade, have been typically reviewed and codified, as shown in Table 2. Recent developments in semiconductor lasers and modulation spectroscopy techniques for methane detection have been described throughout this article. Moreover, some other trends are becoming visible.

Firstly, although QCLs, as convenient mid-infrared laser sources, have not been widely used for commercial detection systems, they may find broad application in mid-infrared modulation spectroscopies in the near future. Then, other wideband-tunable room temperature mid-infrared sources and corresponding mid-infrared technology, such as DFG sources, optical fiber, and detection instruments, will be further developed for trace gas detection. Except for the development of TDLs and

mid-infrared sources, the optimization of optical interference fringe and the formation of multipass cells are observable factors in improving the detection performance. Better sensitivity for methane detection system will be expected when new designs of lasers and multipass cells and methods of suppressing noise are put in operation.

**Author Contributions:** Conceptualization, F.W., and S.J.; investigation, F.W., S.J., Y.W., and Z.T.; Funding acquisition, S.J.; writing—original draft preparation, F.W. and S.J.

**Funding:** This work was supported by the National Natural Science Foundation of China (NSFC) (Grant No. 51575437), the NSFC—Shanxi Provincial Government coal-based low carbon joint fund (Grant No. U1510114), the Key Science and Technology Program of Shaanxi Province of China (Grant No. 2014K07-02) and XJTU University Funding (Grant No. PY3A048).

**Conflicts of Interest:** The authors declare no conflict of interest.

## References

1. Rodhe, H. A comparison of the contribution of various gases to the greenhouse effect. *Science* **1990**, *248*, 1217–1219. [[CrossRef](#)] [[PubMed](#)]
2. Liu, K.; Wang, L.; Tan, T.; Wang, G.; Zhang, W.; Chen, W.; Gao, X. Highly sensitive detection of methane by near-infrared laser absorption spectroscopy using a compact dense-pattern multipass cell. *Sens. Actuators B* **2015**, *220*, 1000–1005. [[CrossRef](#)]
3. Karpov, E.E.; Karpov, E.F.; Suchkov, A.; Mironov, S.; Baranov, A.; Sleptsov, V.; Calliari, L. Energy efficient planar catalytic sensor for methane measurement. *Sens. Actuators A* **2013**, *194*, 176–180. [[CrossRef](#)]
4. Nagai, D.; Nishibori, M.; Itoh, T.; Kawabe, T.; Sato, K.; Shin, W. Ppm level methane detection using micro-thermoelectric gas sensors with Pd/Al<sub>2</sub>O<sub>3</sub> combustion catalyst films. *Sens. Actuators B* **2015**, *206*, 488–494. [[CrossRef](#)]
5. Suzuki, T.; Kunihara, K.; Kobayashi, M.; Tabata, S.; Higaki, K.; Ohnishi, H. A micromachined gas sensor based on a catalytic thick film/SnO<sub>2</sub> thin film bilayer and thin film heater: Part 1: CH<sub>4</sub> sensing. *Sens. Actuators B* **2005**, *109*, 190–193. [[CrossRef](#)]
6. Laan, S.V.D.; Neubert, R.E.M.; Meijer, H.A.J. A single gas chromatograph for accurate atmospheric mixing ratio measurements of CO<sub>2</sub>, CH<sub>4</sub>, N<sub>2</sub>O, SF<sub>6</sub> and CO. *Atmos. Meas. Tech.* **2009**, *2*, 549–559. [[CrossRef](#)]
7. Liu, D.; Fu, S.; Tang, M.; Shum, P.; Liu, D. Comb filter-based fiber-optic methane sensor system with mitigation of cross gas sensitivity. *J. Lightwave Technol.* **2012**, *30*, 3103–3109. [[CrossRef](#)]
8. Lin, H.; Liang, Z.; Li, E.; Yang, M.; Zhai, B. Analysis and design of an improved light interference methane sensor. In Proceedings of the 11th IEEE International Conference on Control & Automation (ICCA), Taiwan, China, 18–20 June 2014.
9. Ma, Y.; He, Y.; Tong, Y.; Yu, X.; Tittel, F.K. Quartz-tuning-fork enhanced photothermal spectroscopy for ultra-high sensitive trace gas detection. *Opt. Express* **2018**, *26*, 32103–32110. [[CrossRef](#)]
10. Leigh, R.J.; Corlett, G.K.; Friess, U.; Monks, P.S. Concurrent multi-axis differential optical absorption spectroscopy system for the measurement of tropospheric nitrogen dioxide. *Appl. Opt.* **2006**, *45*, 7504. [[CrossRef](#)]
11. Rustgi, O.P. Absorption Cross Sections of Argon and Methane between 600 and 170 Å. *JOSA* **1964**, *54*, 464–465. [[CrossRef](#)]
12. Swinehart, D.F. The beer-lambert law. *J. Chem. Educ.* **1962**, *39*, 333–335. [[CrossRef](#)]
13. Kireev, S.V.; Shnyrev, S.L. On-line monitoring of odorant in natural gas mixtures of different composition by the infrared absorption spectroscopy method. *Laser Phys. Lett.* **2018**, *15*. [[CrossRef](#)]
14. Zheng, W.; Zheng, C.; Yao, D.; Yang, S.; Dang, P.; Wang, Y. Development of a mid-infrared interband cascade laser methane sensor. *Acta Opt. Sin.* **2018**, *38*. [[CrossRef](#)]
15. Willer, U.; Saraji, M.; Khorsandi, A.; Geiser, P.; Schade, W. Near- and mid-infrared laser monitoring of industrial processes, environment and security applications. *Opt. Laser Eng.* **2006**, *44*, 699–710. [[CrossRef](#)]
16. Mappé, I.; Joly, L.; Durry, G.; Thomas, X.; Decarpenterie, T.; Cousin, J.; Dumelie, N.; Roth, E.; Chakir, A.; Grillon, P.G. A quantum cascade laser absorption spectrometer devoted to the in situ measurement of atmospheric N<sub>2</sub>O and CH<sub>4</sub> emission fluxes. *Rev. Sci. Instrum.* **2013**, *84*, 222. [[CrossRef](#)]
17. Crosson, E.R. A cavity ring-down analyzer for measuring atmospheric levels of methane, carbon dioxide, and water vapor. *Appl. Phys. B* **2008**, *92*, 403–408. [[CrossRef](#)]

18. Berman, E.S.F.; Fladeland, M.; Liem, J.; Kolyer, R.; Gupta, M. Greenhouse gas analyzer for measurements of carbon dioxide, methane, and water vapor aboard an unmanned aerial vehicle. *Sens. Actuators B* **2012**, *169*, 128–135. [[CrossRef](#)]
19. Gossel, A.; Zéninari, V.; Parvitte, B.; Joly, L.; Courtois, D. Optimization of a compact photoacoustic quantum cascade laser spectrometer for atmospheric flux measurements: Application to the detection of methane and nitrous oxide. *Appl. Phys. B* **2007**, *88*, 483–492. [[CrossRef](#)]
20. Schiff, H.I.; Mackay, G.I.; Bechara, J. The use of tunable diode laser absorption spectroscopy for atmospheric measurements. *Res. Chem. Intermed.* **1994**, *20*, 525–556. [[CrossRef](#)]
21. Kamieniak, J.; Randviir, E.P.; Banks, C.E. Cheminform abstract: The latest developments in the analytical sensing of methane. *Trac Trends Anal. Chem.* **2016**, *47*, 146–157. [[CrossRef](#)]
22. He, Y.; Ma, Y.; Tong, Y.; Yu, X.; Tittel, F.K. Ultra-high sensitive light-induced thermoelastic spectroscopy sensor with a high Q-factor quartz tuning fork and a multipass cell. *Opt. Lett.* **2019**, *44*, 1904–1907. [[CrossRef](#)] [[PubMed](#)]
23. Behera, A.; Wang, A. Calibration-free wavelength modulation spectroscopy: Symmetry approach and residual amplitude modulation normalization. *Appl. Opt.* **2016**, *55*, 4446. [[CrossRef](#)] [[PubMed](#)]
24. Bomse, D.S.; Stanton, A.C.; Silver, J.A. Frequency modulation and wavelength modulation spectroscopies: Comparison of experimental methods using a lead-salt diode laser. *Appl. Opt.* **1992**, *31*, 718–731. [[CrossRef](#)] [[PubMed](#)]
25. Rojas, D.; Jung, P.; Axner, O. An investigation of the 2f-wavelength modulation technique for detection of atoms under optically thin as well as thick conditions. *Spectrochim. Acta Part B* **1997**, *52*, 1663–1686. [[CrossRef](#)]
26. Williams, R.M.; Kelly, J.F.; Sharpe, S.W.; Hartman, J.S.; Gmachl, C.F.; Capasso, F.; Sivco, D.L.; Baillargeon, J.N.; Cho, A.Y. Spectral and modulation performance of quantum cascade lasers with application to remote sensing. *Proc. SPIE* **1999**, *3758*, 11–22.
27. Chan, K.; Ito, H.; Inaba, H. Absorption measurement of  $\nu_2 + 2\nu_3$  band of CH<sub>4</sub> at 1.33  $\mu\text{m}$  using an InGaAsP light emitting diode. *Appl. Opt.* **1983**, *22*, 3802–3804. [[CrossRef](#)] [[PubMed](#)]
28. Schilt, S.; Besson, J.P.; Thévenaz, L. Near-infrared laser photoacoustic detection of methane: The impact of molecular relaxation. *Appl. Phys. B* **2006**, *82*, 319–328. [[CrossRef](#)]
29. Shemshad, J.; Aminossadati, S.M.; Kizil, M.S. A review of developments in near infrared methane detection based on tunable diode laser. *Sens. Actuators B* **2012**, *171–172*, 77–92. [[CrossRef](#)]
30. Tran, H.; Hartmann, J.M.; Toon, G.; Brown, L.R.; Frankenberg, C.; Warneke, T.; Spietz, P.; Hase, F. The  $2\nu_3$  band of CH<sub>4</sub> revisited with line mixing: Consequences for spectroscopy and atmospheric retrievals at 1.67  $\mu\text{m}$ . *J. Quant. Spectrosc. Radiat. Transf.* **2010**, *111*, 1344–1356. [[CrossRef](#)]
31. Gagliardi, G.; Gianfrani, L. Trace-gas analysis using diode lasers in the near-IR and long-path techniques. *Opt. Laser Eng.* **2002**, *37*, 509–520. [[CrossRef](#)]
32. Chan, K.; Ito, H.; Inaba, H. Optical remote monitoring of CH<sub>4</sub> gas using low-loss optical fiber link and InGaAsP light-emitting diode in 1.33- $\mu\text{m}$  region. *Appl. Phys. Lett.* **1983**, *43*, 634–636. [[CrossRef](#)]
33. Chan, K.; Ito, H.; Inaba, H.; Furuya, T. 10 km-long fibre-optic remote sensing of CH<sub>4</sub> gas by near infrared absorption. *Appl. Phys. B* **1985**, *38*, 11–15. [[CrossRef](#)]
34. Washenfelder, R.A.; Wennberg, P.O.; Toon, G.C. Tropospheric methane retrieved from ground-based near-IR solar absorption spectra. *Geophys. Res. Lett.* **2003**, *30*, 2226. [[CrossRef](#)]
35. Gordon, I.E.; Rothman, L.S.; Hill, C.; Kochanov, R.V.; Tan, Y.; Bernath, P.F.; Birk, M.; Boudon, V.; Campargue, A.; Chance, K.V. The HITRAN2016 Molecular Spectroscopic Database. *J. Quant. Spectrosc. Radiat. Transf.* **2013**, *130*, 4–50. [[CrossRef](#)]
36. Gharavi, M.; Buckley, S.G. Diode laser absorption spectroscopy measurement of linestrengths and pressure broadening coefficients of the methane  $2\nu_3$  band at elevated temperatures. *J. Mol. Spectrosc.* **2005**, *229*, 78–88. [[CrossRef](#)]
37. Frankenberg, C.; Warneke, T.; Butz, A.; Aben, I.; Hase, F.; Spietz, P.; Brown, L.R. Pressure broadening in the  $2\nu_3$  band of methane and its implication on atmospheric retrievals. *Atmos. Chem. Phys.* **2008**, *8*, 5061–5075. [[CrossRef](#)]
38. Pine, A.S. N<sub>2</sub> and Ar broadening and line mixing in the P and R branches of the  $\nu_3$  band of CH<sub>4</sub>. *J. Quant. Spectrosc. Radiat. Transf.* **1997**, *57*, 157–176. [[CrossRef](#)]
39. Moorhead, J.G. The near infrared absorption spectrum of methane. *Phys. Rev.* **1932**, *39*, 83–88. [[CrossRef](#)]

40. Pine, A.S. Self, N<sub>2</sub>, O<sub>2</sub>, H<sub>2</sub>, Ar, and He broadening in the  $\nu_3$  band Q branch of CH<sub>4</sub>. *J. Chem. Phys.* **1992**, *97*, 773–785. [[CrossRef](#)]
41. Tran, H.; Flaud, P.M.; Fouchet, T.; Gabard, T.; Hartmann, J.M. Model, software and database for line-mixing effects in the  $\nu_3$  and  $\nu_4$  bands of CH<sub>4</sub> and tests using laboratory and planetary measurements-II: H<sub>2</sub> (and He) broadening and the atmospheres of Jupiter and Saturn. *J. Quant. Spectrosc. Radiat. Transf.* **2006**, *101*, 284–305. [[CrossRef](#)]
42. Mantz, A.W. A review of spectroscopic applications of tunable semiconductor lasers. *Spectrochim. Acta, Part A* **1995**, *51*, 2211–2236. [[CrossRef](#)]
43. Agrawal, G.P.; Dutta, N.K. Laser structures and their performance. In *Long-Wavelength Semiconductor Lasers*; Van Nostrand Reinhold Company: New York, NY, USA, 1986; pp. 172–219.
44. Song, K.; Jung, E.C. Recent Developments in modulation spectroscopy for trace gas detection using tunable diode lasers. *Appl. Spectrosc. Rev.* **2003**, *38*, 395–432. [[CrossRef](#)]
45. Silveira, J.P.; Grasdepot, F. CH<sub>4</sub> optical sensor using a 1.31  $\mu\text{m}$  DFB laser diode. *Sens. Actuators B* **1995**, *25*, 603–606. [[CrossRef](#)]
46. Kogelnik, H.; Shank, C.V. Erratum: Stimulated emission in a periodic structure. *Appl. Phys. Lett.* **1971**, *18*, 408. [[CrossRef](#)]
47. Scifres, D.R.; Burnham, R.D.; Streifer, W. Distributed-feedback single heterojunction GaAs diode laser. *Appl. Phys. Lett.* **1974**, *25*, 203–206. [[CrossRef](#)]
48. Goldenstein, C.S.; Spearrin, R.M.; Jeffries, J.B.; Hanson, R.K. Infrared laser-absorption sensing for combustion gases. *Prog. Energy Combust. Sci.* **2017**, *60*, 132–176. [[CrossRef](#)]
49. Shimose, Y.; Aizawa, M.; Nagai, H. Remote sensing of methane gas by differential absorption measurement using a wavelength tunable DFB LD. *IEEE Photonics Technol. Lett.* **1991**, *3*, 86–87. [[CrossRef](#)]
50. Guenter, J.K.; Amann, M.C.; Arafin, S.; Lei, C.; Vizbaras, K. Single mode and tunable GaSb-based VCSELs for wavelengths above 2  $\mu\text{m}$ . *Proc. SPIE* **2011**, 7952. [[CrossRef](#)]
51. Naehle, L.; Belahsene, S.; Edlinger, M.V.; Fischer, M.; Boissier, G.; Grech, P.; Narcy, G.; Vicet, A.; Rouillard, Y.; Koeth, J.; et al. Continuous-wave operation of type-i quantum well DFB laser diodes emitting in 3.4  $\mu\text{m}$  wavelength range around room temperature. *Electron. Lett.* **2011**, *47*, 46. [[CrossRef](#)]
52. Hosoda, T.; Kipshidze, G.; Shterengas, L.; Belenky, G. Diode lasers emitting near 3.44  $\mu\text{m}$  in continuous-wave regime at 300K. *Electron. Lett.* **2010**, *46*, 1455–1457. [[CrossRef](#)]
53. Tacke, M. New developments and applications of tunable IR lead salt lasers. *Infrared Phys. Technol.* **1995**, *36*, 447–463. [[CrossRef](#)]
54. Werle, P.; Slemr, F.; Gehrtz, M.; Bräuchle, C. Quantum-limited FM-spectroscopy with a lead-salt diode laser. *Appl. Phys. B* **1989**, *49*, 99–108. [[CrossRef](#)]
55. Cassidy, D.T.; Reid, J. Atmospheric pressure monitoring of trace gases using tunable diode lasers. *Appl. Opt.* **1982**, *21*, 1185–1190. [[CrossRef](#)] [[PubMed](#)]
56. Zorabedian, P. Tunable external-cavity semiconductor lasers. In *Tunable Lasers Handbook*; Duarte, F.J., Ed.; Academic Press: San Diego, CA, USA, 1995; pp. 349–442.
57. Liu, A.Q.; Zhang, X.M. A review of mems external-cavity tunable lasers. *J. Micromech. Microeng.* **2007**, *17*, R1–R13. [[CrossRef](#)]
58. Miller, J.H.; Bakhirkin, Y.A.; Ajtai, T.; Tittel, F.K.; Hill, C.J.; Yang, R.Q. Detection of formaldehyde using off-axis integrated cavity output spectroscopy with an interband cascade laser. *Appl. Phys. B* **2006**, *85*, 391–396. [[CrossRef](#)]
59. Li, J.; Parchatka, U.; Fischer, H. A formaldehyde trace gas sensor based on a thermoelectrically cooled CW-DFB quantum cascade laser. *Anal. Methods* **2014**, *6*, 5483–5488. [[CrossRef](#)]
60. Jacoby, M. Quantum cascade lasers. *Chem. Eng. News* **2013**, *88*, 42–43. [[CrossRef](#)]
61. Hancock, G.; Helden, J.H.V.; Peverall, R.; Ritchie, G.A.D.; Walker, R.J. Direct and wavelength modulation spectroscopy using a cw external cavity quantum cascade laser. *Appl. Phys. Lett.* **2009**, *94*. [[CrossRef](#)]
62. Kosterev, A.; Wysocki, G.; Bakhirkin, Y.; So, S.; Lewicki, R.; Fraser, M.; Tittel, F.; Curl, R.F. Application of quantum cascade lasers to trace gas analysis. *Appl. Phys. B* **2008**, *90*, 165–176. [[CrossRef](#)]
63. Tittel, F.K.; Wysocki, G.; Kosterev, A.A.; Bakhirkin, Y.A. Semiconductor Laser Based Trace Gas Sensor Technology: Recent Advances and Applications. In *Mid-Infrared Coherent Sources and Applications*; Ebrahim-Zadeh, M., Sorokina, I.T., Eds.; Springer: Houten, The Netherlands, 2007; pp. 467–493.

64. Taubman, M.S.; Myers, T.L.; Cannon, B.D.; Williams, R.M.; Federico, C.; Claire, G.; Sivco, D.L.; Cho, A.Y. Frequency stabilization of quantum-cascade lasers by use of optical cavities. *Opt. Lett.* **2002**, *27*, 2164–2166. [[CrossRef](#)]
65. Borri, S.; Bartalini, S.; Natale, P.D.; Inguscio, M.; Gmachl, C.; Capasso, F.; Sivco, D.L.; Cho, A.Y. Frequency modulation spectroscopy by means of quantum-cascade lasers. *Appl. Phys. B* **2006**, *85*, 223. [[CrossRef](#)]
66. Rao, G.N.; Andreas, K. External cavity tunable quantum cascade lasers and their applications to trace gas monitoring. *Appl. Opt.* **2011**, *50*, 100–115. [[CrossRef](#)] [[PubMed](#)]
67. Mohan, A.; Wittmann, A.; Hugi, A.; Blaser, S.; Faist, J. Room-temperature continuous-wave operation of an external-cavity quantum cascade laser. *Opt. Lett.* **2007**, *32*, 2792–2794. [[CrossRef](#)] [[PubMed](#)]
68. Kormann, R.; Fischer, H.; Gurk, C.; Helleis, F.; Th, K.; Kowalski, K.; Nigstedt, R.K.; Parchatka, U.; Wagner, V. Application of a multi-laser tunable diode laser absorption spectrometer for atmospheric trace gas measurements at sub-ppbv levels. *Spectrochim. Acta Part A* **2002**, *58*, 2489–2498. [[CrossRef](#)]
69. Paige, M.E.; Silver, J.A.; Petroski, D.; Bomse, D.S. Portable natural gas leak detector for survey inspections. *Proc. SPIE* **2006**, 6378. [[CrossRef](#)]
70. Liang, W.; Bi, Y.; Zhou, Q.; Dong, X.; Lv, T.; Liang, W.; Bi, Y.; Zhou, Q.; Dong, X.; Lv, T. Developing CH<sub>4</sub> detection limit at  $\lambda = 1.654 \mu\text{m}$  by suppressing optical interference fringes in wavelength modulation spectroscopy. *Sens. Actuators B* **2017**, *255*, 2614–2620. [[CrossRef](#)]
71. Huang, J.Q.; Zheng, C.T.; Gao, Z.L.; Ye, W.L.; Wang, Y.D. Near-infrared methane detection device using wavelength-modulated distributed feedback diode laser around  $1.654 \mu\text{m}$ . *Spectrosc. Lett.* **2014**, *47*, 197–205. [[CrossRef](#)]
72. Liu, Y.; Wu, J.N.; Chen, M.M.; Yang, X.H.; Chen, C. The trace methane sensor based on TDLAC-WMS. *Spectrosc. Spectral Anal.* **2016**, *36*, 279–282.
73. Hodgkinson, J.; Tatam, R.P. Optical gas sensing: A review. *Meas. Sci. Technol.* **2013**, *24*, 012004. [[CrossRef](#)]
74. Werle, P.; Slemr, F.; Maurer, K.; Kormann, R.; Mücke, R.; Jänker, B. Near- and mid-infrared laser-optical sensors for gas analysis. *Opt. Lasers Eng.* **2002**, *37*, 101–114. [[CrossRef](#)]
75. Schilt, S.; Thévenaz, L.; Robert, P. Wavelength modulation spectroscopy: Combined frequency and intensity laser modulation. *Appl. Opt.* **2003**, *42*, 6728. [[CrossRef](#)] [[PubMed](#)]
76. Reid, J.; Labrie, D. Second-harmonic detection with tunable diode lasers—Comparison of experiment and theory. *Appl. Phys. B* **1981**, *26*, 203–210. [[CrossRef](#)]
77. Magalhaes, F.; Carvalho, J.P.; Ferreira, L.A.; Araujo, F.M. Methane detection system based on Wavelength Modulation Spectroscopy and hollow-core fibres. In Proceedings of the SENSORS, Lecce, Italy, 26–29 October 2008; pp. 1277–1280.
78. Zheng, C.T.; Huang, J.Q.; Ye, W.L.; Lv, M.; Dang, J.M.; Cao, T.S.; Chen, C.; Wang, Y.D. Demonstration of a portable near-infrared CH<sub>4</sub> detection sensor based on tunable diode laser absorption spectroscopy. *Infrared Phys. Technol.* **2013**, *61*, 306–312. [[CrossRef](#)]
79. Li, B.; Zheng, C.; Liu, H.; He, Q.; Ye, W.; Zhang, Y.; Pan, J.; Wang, Y. Development and measurement of a near-infrared CH<sub>4</sub> detection system using  $1.654 \mu\text{m}$  wavelength-modulated diode laser and open reflective gas sensing probe. *Sens. Actuators B* **2016**, *225*, 188–198. [[CrossRef](#)]
80. Ye, W.L.; Zheng, C.T.; Yu, X.; Zhao, C.X.; Song, Z.W.; Wang, Y.D. Design and performances of a mid-infrared CH<sub>4</sub> detection device with novel three-channel-based LS-FTF self-adaptive denoising structure. *Sens. Actuators B* **2011**, *155*, 37–45. [[CrossRef](#)]
81. Zheng, C.T.; Ye, W.L.; Huang, J.Q.; Cao, T.S.; Lv, M.; Dang, J.M.; Wang, Y.D. Performance improvement of a near-infrared CH<sub>4</sub> detection device using wavelet-denoising-assisted wavelength modulation technique. *Sens. Actuators B* **2014**, *190*, 249–258. [[CrossRef](#)]
82. Shemshad, J. Design of a fibre optic sequential multipoint sensor for methane detection using a single tunable diode laser near 1666 nm. *Sens. Actuators B* **2013**, *186*, 466–477. [[CrossRef](#)]
83. Lackner, M.; Totschnig, G.; Winter, F.W.; Ortsiefer, M.; Roskopf, J. Demonstration of methane spectroscopy using a vertical-cavity surface-emitting laser at  $1.68 \mu\text{m}$  with up to 5 MHz repetition rate. *Meas. Sci. Technol.* **2002**, *14*, 101. [[CrossRef](#)]
84. McDermit, D.; Burba, G.; Xu, L.; Anderson, T.; Komissarov, A.; Riensche, B.; Schedlbauer, J.; Starr, G.; Zona, D.; Oechel, W.; et al. A new low-power, open-path instrument for measuring methane flux by eddy covariance. *Appl. Phys. B* **2011**, *102*, 391–405. [[CrossRef](#)]

85. Ren, W.; Jiang, W.; Tittel, F.K. QCL Based Absorption Sensor for Simultaneous Trace-Gas Detection of CH<sub>4</sub> and N<sub>2</sub>O. *Appl. Phys. B* **2014**, *117*, 245–251. [[CrossRef](#)]
86. Yu, Y.; Sanchez, N.P.; Griffin, R.J.; Tittel, F.K. CW EC-QCL-based sensor for simultaneous detection of H<sub>2</sub>O, HDO, N<sub>2</sub>O and CH<sub>4</sub> using multi-pass absorption spectroscopy. *Opt. Express* **2016**, *24*, 10391–10401. [[CrossRef](#)] [[PubMed](#)]
87. Ye, W.; Li, C.; Zheng, C.; Sanchez, N.P.; Gluszek, A.K.; Hudzikowski, A.J.; Dong, L.; Griffin, R.J.; Tittel, F.K. Mid-infrared dual-gas sensor for simultaneous detection of methane and ethane using a single continuous-wave interband cascade laser. *Opt. Express* **2016**, *24*, 16973–16985. [[CrossRef](#)] [[PubMed](#)]
88. Zheng, C.; Ye, W.; Sanchez, N.P.; Li, C.; Dong, L.; Wang, Y.; Griffin, R.J.; Tittel, F.K. Development and field deployment of a mid-infrared methane sensor without pressure control using interband cascade laser absorption spectroscopy. *Sens. Actuators B* **2017**, *244*, 365–372. [[CrossRef](#)]
89. Dong, L.; Tittel, F.K.; Li, C.; Sanchez, N.P.; Wu, H.; Zheng, C.; Yu, Y.; Sampaolo, A.; Griffin, R.J. Compact TDLAS based sensor design using interband cascade lasers for mid-IR trace gas sensing. *Opt. Express* **2016**, *24*, A528–A535. [[CrossRef](#)] [[PubMed](#)]
90. Armstrong, I.; Johnstone, W.; Duffin, K.; Lengden, M.; Chakraborty, A.L.; Ruxton, K. Detection of in the mid-IR using difference frequency generation with tunable diode laser spectroscopy. *J. Lightwave Technol.* **2010**, *28*, 1435–1442. [[CrossRef](#)]
91. Krzempek, K.; Sobon, G.; Abramski, K.M. DFG-based mid-IR generation using a compact dual-wavelength all-fiber amplifier for laser spectroscopy applications. *Opt. Express* **2013**, *21*, 20023–20031. [[CrossRef](#)] [[PubMed](#)]
92. Krzempek, K.; Soboń, G.; Dudzik, G.; Sotor, J.; Abramski, K.M. Difference frequency generation of Mid-IR radiation in PPLN crystals using a dual-wavelength all-fiber amplifier. *Int. Soc. Opt. Photonics* **2014**, *8964*, 271–283.
93. Zhao, J.; Jia, F.; Feng, Y.; Nilsson, J. Continuous-wave 3.1–3.6 μm difference-frequency generation of dual wavelength-tunable fiber sources in PPMgLN-based rapid-tuning design. *IEEE J. Sel. Top. Quantum Electron.* **2017**, *99*, 1. [[CrossRef](#)]
94. Gao, Q.; Zhang, Y.; Yu, J.; Wu, S.; Zhang, Z.; Zheng, F.; Lou, X.; Guo, W. Tunable multi-mode diode laser absorption spectroscopy for methane detection. *Sens. Actuators A* **2013**, *199*, 106–110. [[CrossRef](#)]
95. Cai, T.; Gao, G.; Wang, M. Simultaneous detection of atmospheric CH<sub>4</sub> and CO using a single tunable multi-mode diode laser at 2.33 μm. *Opt. Express* **2016**, *24*, 859. [[CrossRef](#)]
96. Qi, R.B.; Du, Z.H.; Gao, D.Y.; Li, J.Y.; Xu, K.X. Wavelength modulation spectroscopy based on quasi-continuous-wave diode lasers. *Chin. Opt. Lett.* **2012**, *25*, 77–79.
97. Li, J.; Yu, B.; Zhao, W.; Chen, W. A review of signal enhancement and noise reduction techniques for tunable diode laser absorption spectroscopy. *Appl. Spectrosc. Rev.* **2014**, *49*, 666–691. [[CrossRef](#)]
98. Yang, R.; Dong, X.; Bi, Y.; Lv, T. A method of reducing background fluctuation in tunable diode laser absorption spectroscopy. *Opt. Commun.* **2018**, *410*, 782–786. [[CrossRef](#)]
99. Pilston, R.G.; White, J.U. A long path gas absorption cell. *J. Opt. Soc. Am.* **1954**, *44*, 572–573. [[CrossRef](#)]
100. Herriott, D.; Kogelnik, H.; Kompfner, R. Off-axis paths in spherical mirror interferometers. *Appl. Opt.* **1964**, *3*, 523–526. [[CrossRef](#)]
101. Chernin, S.M.; Barskaya, E.G. Optical multipass matrix systems. *Appl. Opt.* **1991**, *30*, 51–58. [[CrossRef](#)]
102. Xia, J.; Zhu, F.; Zhang, S.; Kolomenskii, A.; Schuessler, H. A ppb level sensitive sensor for atmospheric methane detection. *Infrared Phys. Technol.* **2017**, *86*, 194–201. [[CrossRef](#)]
103. Claude, R. Simple, stable, and compact multiple-reflection optical cell for very long optical paths. *Appl. Opt.* **2007**, *46*, 5408–5418.
104. Kasyutich, V.L. Laser beam patterns of an optical cavity formed by two twisted cylindrical mirrors. *Appl. Phys. B: Lasers Opt.* **2009**, *96*, 141–148. [[CrossRef](#)]
105. Ofner, J.; Heinz-Ulrich, K.; Zetzsch, C. Circular multireflection cell for optical spectroscopy. *Appl. Opt.* **2010**, *49*, 5001. [[CrossRef](#)]
106. Bjorklund, G.C. Frequency-modulation spectroscopy: A new method for measuring weak absorptions and dispersions. *Opt. Lett.* **1980**, *5*, 15. [[CrossRef](#)] [[PubMed](#)]
107. Zhang, L.; Tian, G.; Li, J.; Yu, B. Applications of absorption spectroscopy using quantum cascade lasers. *Appl. Spectrosc.* **2014**, *68*, 1095–1107. [[CrossRef](#)] [[PubMed](#)]

108. Silver, J.A. Frequency-modulation spectroscopy for trace species detection: Theory and comparison among experimental methods: Errata. *Appl. Opt.* **1992**, *31*, 4927. [[CrossRef](#)] [[PubMed](#)]
109. Osterwalder, J.M.; Rickett, B.J. Frequency modulation of GaAlAs injection lasers at microwave frequency rates. *IEEE J. Quantum Electron.* **1980**, *16*, 250–252. [[CrossRef](#)]
110. Güllük, T.; Wagner, H.E.; Slemr, F. A high-frequency modulated tunable diode laser absorption spectrometer for measurements of CO<sub>2</sub>, CH<sub>4</sub>, N<sub>2</sub>O, and CO in air samples of a few cm<sup>3</sup>. *Rev. Sci. Instrum.* **1997**, *68*, 230–239. [[CrossRef](#)]
111. Van Well, B.; Murray, S.; Hodgkinson, J.; Pride, R.; Strzoda, R.; Gibson, G.; Padgett, M. An open-path, hand-held laser system for the detection of methane gas. *J. Opt. A: Pure Appl. Opt.* **2005**, *7*, S420–S424. [[CrossRef](#)]
112. Uehara, K.; Tai, H. Remote detection of methane with a 1.66-microm diode laser. *Appl. Opt.* **1992**, *31*, 809–814. [[CrossRef](#)]
113. Iseki, T.; Tai, H.; Kimura, K. A portable remote methane sensor using a tunable diode laser. *Meas. Sci. Technol.* **2000**, *11*, 594. [[CrossRef](#)]
114. Gagliardi, G.; Borri, S.; Tamassia, F.; Capasso, F.; Gmachl, C.; Sivco, D.L.; Baillargeon, J.N.; Hutchinson, A.L.; Cho, A.Y. A frequency-modulated quantum-cascade laser for spectroscopy of CH<sub>4</sub> and N<sub>2</sub>O isotopomers. *Isotopes. Environ. Health. Stud.* **2005**, *41*, 313–321. [[CrossRef](#)]
115. Chen, G.; Martini, R.; Park, S.W.; Bethea, C.G.; Chen, I.C.A.; Grant, P.D.; Dudek, R.; Liu, H.C. Optically induced fast wavelength modulation in a quantum cascade laser. *Appl. Phys. Lett.* **2010**, *97*. [[CrossRef](#)]
116. Eichholz, R.; Richter, H.; Wienold, M.; Schrottke, L.; Hey, R.; Grahn, H.T.; Hübers, H.W. Frequency modulation spectroscopy with a THz quantum-cascade laser. *Opt. Express* **2013**, *21*, 32199–32206. [[CrossRef](#)]
117. Hübers, H.W.; Pavlov, S.G.; Richter, H.; Semenov, A.D.; Mahler, L.; Tredicucci, A.; Beere, H.E.; Ritchie, D.A. High-resolution gas phase spectroscopy with a distributed feedback terahertz quantum cascade laser. *Appl. Phys. Lett.* **2006**, *89*. [[CrossRef](#)]
118. Cassidy, D.T.; Reid, J. Harmonic detection with tunable diode lasers—Two-tone modulation. *Appl. Phys. B* **1982**, *29*, 279–285. [[CrossRef](#)]
119. Janik, G.R.; Carlisle, C.B.; Gallagher, T.F. Two-tone frequency-modulation spectroscopy. *J. Opt. Soc. Am. B* **1986**, *3*, 1070–1074. [[CrossRef](#)]
120. Cooper, D.E.; Warren, R.E. Frequency modulation spectroscopy with lead-salt diode lasers: A comparison of single-tone and two-tone techniques. *Appl. Opt.* **1987**, *26*, 3726–3732. [[CrossRef](#)]
121. Modugno, G.; Corsi, C.; Gabrysch, M.; Marin, F.; Inguscio, M. Fundamental noise sources in a high-sensitivity two-tone frequency modulation spectrometer and detection of CO<sub>2</sub> at 1.6 μm and 2 μm. *Appl. Phys. B* **1998**, *67*, 289–296. [[CrossRef](#)]
122. Maddaloni, P.; Malara, P.; Gagliardi, G.; Natale, P.D. Two-tone frequency modulation spectroscopy for ambient-air trace gas detection using a portable difference-frequency source around 3 μm. *Appl. Phys. B* **2006**, *85*, 219–222. [[CrossRef](#)]

